AD-A013 009

NUMERICAL SOLUTION TO THE OPTIMAL CONTROL OF A GLIDING PARACHUTE SYSTEM

Kuang-Chung Wei, et al

Brown University

Prepared for:

Army Natick Laboratories

October 1974

SECURITY CLASSIFICATION OF THIS PAGE (When Date Entered)

REPORT DOCUMENTATION PAGE

READ INSTRUCTIONS BEFORE COMPLETING FORM

1. REPORT NUMBER	2. GOVT ACCESSION NO.
3. RECIPIENT'S CATALOG NUMBER	AD-A013 004
4. TITLE (and Subtitle) NUMERICAL SOLUTION TO THE OPTIMAL CONTROL OF A GLIDING PARACHUTE SYSTEM	5. TYPE OF REPORT & PERIOD COVERED Interim June 1973 - June 1974
	6. PERFORMING ORG. REPORT NUMBER
7. AUTHOR(s) Kuang-Chung Wei and Allan E. Pearson	8. CONTRACT OR GRANT NUMBER(s) DAAG-17-73-C-0172
9. PERFORMING ORGANIZATION NAME AND ADDRESS Division of Engineering and Lefschetz Center for Dynamical Systems - Brown University, Providence, Rhode Island 02912	10. PROGRAM ELEMENT, PROJECT, TASK AREA & WORK UNIT NUMBERS 62203A 1F262203AH86 04 031
11. CONTROLLING OFFICE NAME AND ADDRESS US Army Natick Development Center Aero-Mechanical Engineering Laboratory AMXNM-UE Natick, Massachusetts 01760	12. REPORT DATE October 1974
	13. NUMBER OF PAGES
14. MONITORING AGENCY NAME & ADDRESS (if different from Controlling Office)	15. SECURITY CLASS. (of this report) Unclassified
	15a. DECLASSIFICATION/DOWNGRADING SCHEDULE

16. DISTRIBUTION STATEMENT (of this Report)

Approved for public release; distribution unlimited.

17. DISTRIBUTION STATEMENT (of the abstract entered in Block 20, if different from Report)

This document has been approved for public release and sale; its distribution is unlimited.

18. SUPPLEMENTARY NOTES

19. KEY WORDS (Continue on reverse side if necessary and identify by block number)

Decelerator
Parachute
Optimal Control
Control Theory

PRICES SUBJECT TO CHANGE

20. ABSTRACT (Continue on reverse side if necessary and identify by block number)

This study is concerned with an optimal control policy for the problem of minimizing control energy and the terminal missed distance from a target at touchdown of a gliding parachute system. The bank angle of the parachute is considered as a control variable. Under the condition of a uniform wind, a systematic search on the horizontal normalized plane is completed. A certain region is computed and specified within which a feasible control solution has been found using a specific numerical scheme. The numerical method is based on a second order differential dynamic programming algorithm due to K. Mårtensson.

DD FORM 1 JAN 73 1473 EDITION OF 1 NOV 65 IS OBSOLETE

SECURITY CLASSIFICATION OF THIS PAGE (When Data Entered)

PREFACE

This report was prepared under contract with Brown University in the Division of Engineering and Lefschetz Center for Dynamical Systems. This work was carried out under Exploratory Development Project 1F262203AH86, Control of Gliding Parachute Systems, for the U.S. Army Natick Laboratories, Natick, Massachusetts. Mr. Arthur L. Murphy, Jr., of the Engineering Science Division, Aero-Mechanical Engineering Laboratory, at the U.S. Army Natick Laboratories, was the Project Engineer for this effort.

The authors wish to express their appreciation to Dr. K. Mårtensson of Lund Institute of Technology, Sweden, for his generous supply of the computer program and advice on this work.

TABLE OF CONTENTS

LIST OF TABLES

LIST OF FIGURES

I. INTRODUCTION

Given a nonlinear parachute gliding system, control can be effected by a servomotor pulling on the shroud lines of the parachute which causes a banked turn of the parachute and a change in the direction of flight. Under the condition that the magnitude of the wind velocity vector $\bar{w}$ be less than that of the parachute horizontal velocity vector $\bar{v}$ (relative to air); i.e., $||\bar{w}|| < ||\bar{v}||$, the parachute possesses a wind penetrating capability and the potential of reaching the target under arbitrary wind directions. It is assumed that the initial altitude, and thus the gliding period, is properly chosen in accordance with the wind angle θ and the ratio $||\bar{w}||/||\bar{v}||$ such that a solution exists. Also, a uniform wind, constant in both magnitude and direction, is assumed throughout this analysis.

It is desired to compute a control law which minimizes the control effort and the terminal error from the target. The usual linearization analysis is insufficient to approximate the given system due to the highly transcendental nonlinearities. Thus, a numerical solution to this problem is developed and intended to give some light to the stochastic wind case study. The numerical algorithm derived by Mårtensson [4] in solving the Hamilton-Jacobi-Bellman partial differential equation with the differential dynamic programming (DDP) principle is applied to solve the given nonlinear gliding problem. The theoretical derivation of this algorithm is given in the Appendix.

II. PROBLEM FORMULATION

A. System Equations and Transformation

Assuming a constant wind $\bar{w}$ with angle θ in the horizontal plane, a constant rate of descent v, and an initial altitude h_o at launch time, the equations of motion governing the parachute can be expressed in the horizontal plane as follows: (Pearson [5])

$$\frac{d}{dt}\bar{p} = \bar{v} + \bar{w} \qquad 0 \leq t \leq T \equiv \frac{h_o}{v} \tag{1}$$

$\bar{p}$: position vector

$\bar{v}$: horizontal velocity of parachute relative to air.

This is depicted in Fig. 1. The velocity vector $\bar{v}(t)$ is assumed to have constant magnitude a. Thus $\bar{v}$ can be represented by

$$\begin{aligned} v_1(t) &= a \cos[\omega(t)] \\ v_2(t) &= a \sin[\omega(t)] \end{aligned} \tag{2}$$

where the velocity angle $\omega(t)$ is related to the bank angle ϕ of the parachute via the well-known relation

$$\frac{d}{dt}\omega(t) = \frac{g}{a}\tan\phi(t) \tag{3}$$

g: gravity acceleration.

Since the bank angle ϕ can be directly manipulated by changes in the servomotor connecting the shroud lines, we can rewrite eq. (1) - (3) as

$$\begin{aligned} \frac{d}{dt}p_1 &= a\cos\omega + w_1 \\ \frac{d}{dt}p_2 &= a\sin\omega + w_2 \\ \frac{d}{dt}\omega &= u \end{aligned} \tag{4}$$

in which u is regarded as the control variable. Let $\bar{p}(t_o)$, $\omega(t_o)$, and $\bar{w}(t_o)$ be given at some initial time t_o in the interval $0 < t_o < T$. A performance index which takes into account several desirable features of this problem is

$$P(u) = \frac{1}{2}||p(T)||^2 + \frac{1}{2}c\,[\omega(T)-\theta-\pi]^2 + \frac{q_2}{2(T-t_o)}\int_{t_o}^{T} u^2(t)dt \tag{5}$$

where q_1 and q_2 are non-negative weighting parameters. In eq. (5) the first term, $1/2\ ||p(T)||^2$, reflects the desirability of minimizing the Euclidean distance from the target at the predetermined terminal time T. The second term reflects the desirability of having the parachute point upwind at the terminal time in order to reduce the net horizontal velocity and thus the impact at touchdown. The last term reflects the cost of control effort in terms of the 'average power' spent over the interval $t_o \leq t \leq T$.

A time-varying transformation of the origin could be made according to

$$\bar{y} \equiv \bar{p} + (T-t)\bar{w} \qquad t_o \leq t \leq T \tag{6}$$

Then minimizing $||\bar{p}(T)||$ is equivalent to minimizing $||\bar{y}(T)||$. Moreover, the independent variable t could be transformed via

$$\tau \equiv \frac{t-t_o}{T-t_o} \tag{7}$$

Define a set of new variables x_1, x_2, x_3 by

$$x_1 = \frac{y_1}{a(T-t_o)}, \qquad x_2 = \frac{y_2}{a(T-t_o)}, \qquad x_3 = \omega \tag{8}$$

The system equations after transformation become

$$\begin{aligned} \dot{x}_1 &= \cos x_3 \\ \dot{x}_2 &= \sin x_3 \qquad\qquad 0 \leq \tau \leq 1 \\ \dot{x}_3 &= (T-t_o)u \equiv \hat{u} \end{aligned} \tag{9}$$

with initial conditions

$$\begin{aligned} x_1(0) &= \frac{1}{a(T-t_o)}\,[p_1(t_o) + (T-t_o)w_1] \\ x_2(0) &= \frac{1}{a(T-t_o)}\,[p_2(t_o) + (T-t_o)w_2] \\ x_3(0) &= \omega(t_o) \end{aligned}$$

Here '·' denotes differentiation with respect to normalized time τ. The performance index in terms of these new variables can be rewritten as

$$\hat{P}(\hat{u}) = x_1^2(1) + x_2^2(1) + Q_1[x_3(1)-\theta-\pi]^2 + Q_2 \int_0^1 \hat{u}^2(\tau)d\tau \qquad (10)$$

$$Q_1 \equiv \frac{q_1}{a^2(T-t_o)^2} \qquad Q_2 \equiv \frac{q_2}{a^2(T-t_o)^4}$$

In vector form we have

$$\dot{x} = A(x) + B\hat{u} \qquad (11)$$

$$\hat{P}(\hat{u}) = \int_0^1 [A^o(x) + B^o(\hat{u},t)]dt \qquad (12)$$

where

$$A(x) = \begin{bmatrix} \cos x_3 \\ \sin x_3 \\ 0 \end{bmatrix}, \quad B = \begin{bmatrix} 0 \\ 0 \\ 1 \end{bmatrix}$$

$$A^o(x) = x_1^2(1) + x_2^2(1) + Q_1[x_3(1)-\theta-\pi]^2$$

$$B^o(\hat{u},t) = Q_2\hat{u}^2(t) .$$

B. Existence of Optimal Control

According to an existence theorem by Lee and Markus [3], we can show the existence of an optimal control to our problem.

Theorem 2.1: Consider the following process in R^n:

$$\dot{x} = A(x,t) + B(x,t)u \qquad 0 \leq t \leq T$$

A performance index

$$P(u) = \int_0^T [A^o(x,t) + B^o(u,t)]dt$$

is to be minimized.

Assume:

(i) A, B, A^o, B^o, $\frac{\partial A}{\partial x}$, $\frac{\partial B}{\partial x}$ are continuous for all $x \in R^n$, $u \in R^m$, $t \in R$

(ii) $A^o(x,t) \geq 0 \quad \forall (x,t) \in R^{n+1}$

(iii) $B^o(u,t) \geq m|u|^p$ for some constant $m > 0$, $p > 1$

(iv) For each fixed t, $B^o(u,t)$ is convex in u

(v) $|x(t)| \leq \beta(|u|_1)$, where $\beta(\cdot)$ is a monotonic increasing function.

($|\cdot|_1$ expresses L_1-norm).

Let the set of admissible controls be $L_p[0,T]$ such that the response x(t) initiating at x_o yields a finite P(u). Then there exists an optimal control u* which minimizes P(u).

Proof Refer to [3].

In view of eqs. (11) and (12), conditions (i) thru (iv) are evidently satisfied. Let

$$|x(t)| = \sum_{i=1}^{3} |x_i(t)| \qquad 0 \leq t \leq 1 \tag{13}$$

Since

$$x_1(t) = x_1(o) + \int_o^t \cos[x_3(s)]ds$$

it follows from the triangle inequality that

$$|x_1(t)| \leq |x_1(o)| + \int_o^t |\cos[x_3(s)]|ds \leq |x_1(o)| + 1.$$

Similarly,

$$|x_2(t)| \leq |x_2(o)| + 1$$

and

$$|x_3(t)| \leq |x_3(o)| + \int_o^1 |\hat{u}(s)|ds = |x_3(o)| + |\hat{u}(t)|_1 .$$

Substituting these inequalities into eq. (13),

$$|x(t)| \leq 2 + \sum_1^3 x_i(o) + |\hat{u}(t)|_1 \equiv \beta(|\hat{u}(t)|_1) .$$

Obviously, $\beta(\cdot)$ is monotonically increasing in its argument; thus, condition (v) is also fulfilled. By Theorem 2.1 there exists an optimal control $u^* \in L_2[o,1]$ which minimizes the performance index $\hat{P}(\hat{u})$.

C. Necessary Conditions for Terminal Constraint Problem

A more appealing problem is to incorporate the terminal constraints into the original optimization problem, i.e., to consider the following modified performance index:

$$\tilde{P}(\hat{u}) = x_1^2(1) + x_2^2(1) + Q_1[x_3(1)-\theta-\pi]^2 + b_1x_1(1) + b_2x_3(1)$$
$$+ b_3[x_3(1)-\theta-\pi] + Q_2\int_o^1 \hat{u}^2(s)ds \qquad (14)$$

b_i's are appropriate Lagrange multipliers.

In this constrained optimization formulation, we require that the parachute be driven to the target and directed opposite to the wind at touchdown, while the average energy spent is minimized. Recall the integral form of the system equations

$$x_1(t) = x_1(o) + \int_o^t \cos[x_3(s)]ds$$
$$x_2(t) = x_2(o) + \int_o^t \sin[x_3(s)]ds \qquad 0 \leq t \leq 1 \qquad (15)$$

By the Schwartz inequality,

$$|x_1(t) - x_1(o)|^2 \leq \{\int_o^t |\cos[x_3(s)]|ds\}^2 \leq \int_o^t \cos^2[x_3(s)]ds$$
$$|x_2(t) - x_2(o)|^2 \leq \int_o^t \sin^2[x_3(s)]ds \ .$$

This implies

$$|x_1(1) - x_1(o)|^2 + |x_2(1) - x_2(o)|^2 \leq 1 \ .$$

Hence, if a control exists which drives x_1 and x_2 to the origin at the terminal time, it is necessary that

$$|x_1(o)|^2 + |x_2(o)|^2 \leq 1$$

In other words, the initial conditions of x_1 and x_2 must lie within the unit circle on the horizontal normalized plane.

One other observation is that if we negate the trajectory of x_3 by applying a negative control and a negative initial condition on x_3, the system equations become

$$-x_3(t) = -x_3(o) + \int_o^t [-\hat{u}(s)]ds$$

$$-x_2(t) = -x_2(o) + \int_o^t \sin[-x_3(s)]ds$$

$$x_1(t) = x_1(o) + \int_o^t \cos[-x_3(s)]ds$$

Due to the symmetric property of the cosine function, we conclude that it is sufficient to consider the upper half unit circle as the working zone of our problem. This is shown in Fig. 2. The negation of an optimal control u* for a set of initial conditions $(x_1(o), x_2(o), x_3(o))$ would be an optimal control for the set of initial conditions $(x_1(o), -x_2(o), -x_3(o))$.

III. COMPUTER SIMULATION

The purpose of this simulation work is to study the practicality of computing an optimal control on-line with the DDP algorithm. Given a uniform wind with known magnitude and direction, a constant descent rate, initial altitude and direction of the parachute velocity vector relative to air, selected points in the upper unit circle are chosen with various launching angle $\omega(o)$ to initiate a search for the optimal control as a function of time. Since the initial guess of the nominal control and multipliers plays a crucial role in the convergence, in order to make a proper correction of an initial guess promptly after the first one fails, the entire simulations have been executed under a time-sharing system CP/CMS of IBM/360.

A. Simulation Procedure

In accordance with the DDP algorithm described in the Appendix, an outline of the simulation procedure is as follows:

1. Guess a nominal control $\bar{u}(t)$, $0 \leq t \leq 1$, and integrate the system equations to obtain $\bar{x}(t)$. Store $\bar{u}(t)$, $\bar{x}(t)$. Guess a set of nominal multipliers $\bar{b}$, and compute the corresponding nominal cost $\bar{V}(x_o,\bar{b},0)$.

2. Compute boundary conditions for "a", V_x, and V_{xx}, then integrate $\dot{a}$, $\dot{V}_x$, $\dot{V}_{xx}$ backwards from t = 1 to t = 0, while minimizing $H(\bar{x},u,V_x,t)$. Compute β_1 and store the minimizing control $u^*(t)$, β_1, and $a(\bar{x},\bar{b},t)$.

3. Compare $|a(x_o,\bar{b},0)|$ with a specified small quantity η_1. If $|a| < \eta_1$, the predicted change in the performance index is small; $(\bar{u},\bar{x})$ thus is considered as the optimal solution of a constraint-free problem. Otherwise, go to 4.

   In addition, if $||\psi(x(1),1)|| < \eta_2$, where η_2 is a specified allowable terminal error, then $(\bar{u},\bar{x},\bar{b})$ is considered as the optimal solution of the terminal constraint problem. Stop.

4. Apply the modified control $u = u^* + \beta_1(x-\bar{x})$ from t = 0 to t = 1. If the reduction in cost, $\bar{V}-V$, is large enough compared with the predicted change in cost; e.g., $\frac{\bar{V}-V}{|a|} > c$ ($\simeq 0.5$), c is an empirical factor, then let (u,x) be the new nominal solution and go to 2. Otherwise, 'step-size adjustment' technique is required. (Jacobson and Mayne [2])

5. Modify the multipliers by δb so that $F + (\bar{b} + \delta b)'\psi + \int_o^1 L ds$ attains a minimum corresponding to $\psi = 0$. Then compute boundary conditions for V_b, V_{xb}, V_{bb}. Integrate $\dot{V}_b$, $\dot{V}_{xb}$, $\dot{V}_{bb}$ backward from t = 1 to t = 0. Compute β_2, and store it.

6. To compute δb, notice that for the optimal solution

   $$V_b(x_o,b^*,0) = \psi'(x^*(1),1) = 0 \quad \text{where} \quad b^* = \bar{b} + \delta b .$$

   Expand V_b to first order about $\bar{b}$ and assume $V_{bb}(x_o,\bar{b},0)$ is nonsingular; we have

$$\delta b = -V_{bb}^{-1}(x_o,\bar{b},0)V_b'(x_o,\bar{b},0)$$

7. Apply the new control $u = u^* + \beta_1\delta x + \beta_2\delta b$ to the system. Store u and x, then check whether δb is acceptable or not according to

   (i) $||\psi(\tilde{x}(1),1)|| - ||\psi(x(1),1)|| > 0$

   (ii) $\gamma_2 > \dfrac{\tilde{V}(x_o,b^*,0) - \bar{V}(x_o,\bar{b},0)}{V(x_o,b^*,0) - \bar{V}(x_o,\bar{b},0)} > \gamma_1$

   where $\tilde{V}$ is the new nominal cost, γ_1 and γ_2 are suitably chosen (e.g., $0 < \gamma_1 < 1$, $\gamma_2 > 1$). If satisfied, (u,x) is a new improved nominal solution with cost $\tilde{V}$. Return to 2. If not, go to 8.

8. Choose $(\delta b)_{new} = \frac{1}{2}\delta b$ and go to 7. If no correction has been attained after several reductions of δb, then (ii) of 7 is released. The only demand on δb is to reduce $||\psi||$.

B. Simulation Results

In Section II.B we have shown that it is sufficient to consider the upper half unit circle as a working zone. Twelve rays of angles 0°, 14°, 30°, 45°, 68.2°, 90°, 105°, 120°, 135°, 150°, 165° and 180° partition the upper-half unit circle into eleven sectors. Five points are chosen along each ray as initial launching points. They are located at 0.1, 0.35, 0.6, 0.8 and 0.95 of the unit radius and expressed as A, B, C, D, E, respectively. It is assumed that the complete feasible region is so smooth that the distribution pattern over these sixty points is enough to represent the upper half unit circle. Table 1 lists the coordinates of these points.

Without loss of generality, an easterly wind (along the negative x_1-axis) is considered of magnitude 20 ft/sec. The magnitude of the parachute velocity relative to air is 30 ft/sec. An error criterion of 0.015 is considered in the

iterative process, which allows maximum deviation from the target at touchdown of no more than 45 ft. and deviation from the up-wind direction of no more than 8.5°. Weighting factors Q_1 and Q_2 are 1.0 and 0.1, respectively. The gliding time is 100 sec.; however, only normalized time appears in the simulation process. The unit time interval is once divided into 100 subintervals when an integration routine is applied, although the DDP algorithm is originally devised to equip the integration routine with 500 subintervals. By taking this subdivision it is found that only one-fourth of computer storage (128K bytes) and one-third of cost are required in addition to a loss of accuracy within an order of 1% compared to that of '500' subdivision.

Based on the information available before the search, different initial guesses of nominal control and multipliers are used. Among these, constant control with null multipliers as well as piecewise constant control with null multipliers are interchangeably chosen for every initial setting of launching angle. The value of the control is determined such that the launching angle is driven opposite to the wind at the terminal time by this control. In addition, for each fixed radial point consecutive changes of launching angle are made to form a complete data set. At each step change of these angles, a previous successful optimal control and multipliers are considered as current initial guesses of the nominal control and multipliers. In most instances, as one would expect, the latter combination achieves much better convergence than the former two.

It is observed that as far as the convergence is concerned, there is a strong dependence on the way launching angle is measured. More specifically, if we define a counterclockwise measurement to be positive, then a convergent solution is achieved more frequently for a negative launching angle than for its positive counterpart (i.e., $\omega_o + 2\pi$). This can be seen from the fact that the velocity angle is directly effected by control and the wind is pointed along the

negative x_1-axis which requires the terminal velocity angle to be zero. A negative measure of launching angle directs the trajectory to make a counterclockwise turn towards the wind at the terminal time. For instance, consider a test point A in the first quadrant with a launching angle $-\pi$ or its counterpart π. We can plot a tentative optimal trajectory initiated by $-\pi$ as the dotted line, the trajectory initiated by π as the circled line shown in Fig. 3. It is clear from this figure that the dotted trajectory is much more feasible than the circled one. In this case a negative launching angle with a positive control which gives a counterclockwise turn towards the wind has a better potential to reach the origin than a trajectory initiated by a positive launching angle. Similar situations are illustrated at test points B and C. This geometrical consideration determines an initial guess of the nominal control which usually results in a convergent solution.

Representative optimal controls and corresponding trajectories in the normalized plane are shown in Fig. 4 thru Fig. 8. Since an easterly wind is considered, the velocity angle is driven to zero at the terminal time. This is easily seen from these figures by noting that the slope of x_1-x_2 trajectory denotes the tangent of the velocity angle. For those points outside 80% of the unit circle, the optimal control renders most of its effort (in terms of magnitude) to bend the trajectory at the beginning towards a natural glide (i.e., with null control) and to the opposite direction of wind at the end of flight. If a bank angle restriction were imposed in a practical case, which means the control is constrained to a certain bounded value, then a prolonged gliding period, which in turn requires a higher launching altitude, has to be used in place of the 100 sec. considered here to scale the magnitude of this control, see eq. (9).

It is also interesting to notice that for some of these test points, the magnitude of launching angle is even raised beyond 300° in order to achieve a convergent solution. This trend becomes more apparent as the test points move

along a radial direction towards the origin. Meanwhile, the optimal control pattern appears to exhibit low frequency sinusoidal characteristics. In other words, the control effort is smoothed throughout the whole time interval rather than sharply enforced at the beginning and end of flight. The reason is that the closer the test point to the origin, the more effort should be spent to counterbalance the trade-off between the fixed gliding time and distance from the origin. Thus the optimal trajectory has a somersault turning effect; i.e., for those circumstances where the excess flight time is large the parachute meanders around the target.

In the simulation process, it is felt that a good choice of Lagrange multipliers in addition to the nominal control usually makes a distinct difference to the final convergence. The self-adjustment routines provided by the DDP algorithm in computing the improved variation of multipliers and control are based on a second order Taylor expansion about the optimal solutions. The optimal multipliers corresponding to the optimal solutions depicted in Fig. 4 thru Fig. 8 are given in Table 2. From this, one can sketch how sensitive these multipliers are to the initial condition changes.

The entire simulation work is summarized in Fig. 9. Completely and partially feasible regions are specified individually as the pear shape shaded area and funnel shape spots outside this area. This map provides a convenient reference for the pilot to drop the parachute while flying into the completely feasible region under uniform wind condition. All feasible ranges of launching angle are tabulated in Table 3. The bank angles corresponding to the magnitudes of the normalized controls are shown in Fig. 10 for various $(T-t_o)$ values. A comparison with the optimal control values in Figs. 4-8 indicates that bank angles exceeding 30° would only be required when the time to go is relatively short -- on the order of 20 or 30 seconds.

An average cost of $2.50 corresponding to a CPU time of 20 sec. is needed to compute a typical solution.

IV. CONCLUSION AND REMARKS

The optimal control problem for a gliding parachute system is formulated in two ways. One is to minimize the performance index without terminal constraints, and the other is with the constraint. We have shown the existence of an optimal control for the former problem. Nevertheless, we can only provide some convergent results in the latter case. Two reasons may explain this. First, the controllability question of a nonlinear system of the type considered here is not answered yet; that is, the existence of such a control that drives the given system to the origin at a prespecified time is beyond our knowledge. Second, an inherent deficiency in the DDP successive approximation scheme arises when singular matrix inversions are encountered.

A completely feasible region in the upper half unit circle is computed and specified. In this region, a convergent solution is achieved for any given condition. In the rest of the upper unit circle, for different initial coordinates (x_1, x_2), feasible ranges of launching angle from which convergent solutions are obtained have also been specified.

It is observed that the optimal control function, as well as the feasible range of launching angle, varies considerably along both the radial and circular direction. The initial guess of nominal control and multipliers thus plays an important role in obtaining convergence. In most cases, a geometrical consideration is helpful to determine such an initial guess.

From a practical viewpoint, further investigation is needed to determine either a more efficient algorithm for computing optimal controls or an acceptable suboptimal control law which can be implemented on-line.

References

1. Bryson, A. E., Ho, Y. C., "Applied Optimal Control", Blaisdell, Waltham, 1969.

2. Jacobson, D. H., Mayne, D. Q., "Differential Dynamic Programming", American Elsevier Publishing Company, New York, 1970.

3. Lee, E. B., Markus, L., "Foundation of Optimal Control Theory", New York, Wiley, 1967.

4. Mårtensson, K., "New Approaches to the Numerical Solution of Optimal Control Problem", Report 7206, Division of Automatic Control, Lund Institute of Technology, March 1972.

5. Pearson, A. E., "Optimal Control of a Gliding Parachute System", Technical Report 73-30-AD, August 1972, USA Natick Laboratories, Natick, MA.

AEP/llt
6/75

APPENDIX

Derivation of a DDP algorithm

A second order differential dynamic programming (DDP) algorithm is applied to compute the optimal control for selected initial conditions in the upper half unit circle. Here is a brief review of the derivation of this algorithm. (Martensson [4])

Given a dynamic system

$$\dot{x} = f(x, u, t) \qquad x(0) = x_o \ . \tag{16}$$

and the performance index

$$\min_{\substack{u(t) \\ 0 \le t \le T}} J(u) = \min_{\substack{u(t) \\ 0 \le t \le T}} \left\{ F[x(T),T] + \int_o^T L(x,u,t)dt \right\} \tag{17}$$

subject to the constraint equation

$$\psi[x(T),T] = 0 \ . \tag{18}$$

One way to manage the terminal constraints is to incorporate ψ into the performance index by means of Lagrange multipliers (Bryson and Ho [1]). From now on, we will consider the modified performance index

$$\hat{J}(u) = F[x(T),T] + \int_o^T L(x,u,t)dt + b' \psi [x(T),T] \tag{19}$$

($'$) means taking the transpose of a vector or matrix.)

Define

$$V(x,b,t) \equiv \min_{\substack{u(s) \\ t \le s \le T}} \left\{ F + b' \psi + \int_t^T L ds \right\} \tag{20}$$

Assuming that $V(x,b,t)$ exists and is twice continuously differentiable with respect to x and t for all $t\varepsilon[0,T]$, then V satisfies the Hamilton-Jacobi-Bellman equation

$$-\frac{\partial V}{\partial t} = \min_{u} \left\{L + V_x f\right\} \tag{21}$$

Suppose $\bar{u}$, $\bar{x}$, $\bar{b}$ is a nominal solution neighboring to the optimal solution $u^*(t) = \bar{u}(t) + \delta u(t)$, $x^*(t) = \bar{x}(t) + \delta x(t)$, $b^* = \bar{b} + \delta b$ then equation (21) becomes

$$-\frac{\partial V}{\partial t}(x^*,b^*,t) = \min_{\delta u} \{L(\bar{x} + \delta x,\bar{u} + \delta u, t) + V_x(\bar{x} + \delta x, \bar{b} + \delta b, t) f(\bar{x} + \delta x, \bar{u} + \delta u, t) \tag{22}$$

Now assume $V(x^*, b^*, t)$ is sufficiently smooth to be expanded in a second order Taylor expansion. Then we can approximate $V(x^*, b^*, t)$ with

$$V(x^*, b^*, t) = V + V_x\delta x + V_b\delta b + \langle\delta x, V_{xb}\delta b\rangle + \frac{1}{2}\langle\delta x, V_{xx}\delta x\rangle + \frac{1}{2}\langle\delta b, V_{bb}\delta b\rangle$$

$$V_x(x^*, b^*, t) = V_x + \delta x' V_{xx} + \delta b' V_{xb} \tag{23}$$

all quantities are evaluated at $\bar{x}$, $\bar{b}$, t unless otherwise specified. Let $a(\bar{x}, \bar{b}, t)$ be the difference between optimal cost at $\bar{x}$, $\bar{b}$, t and predicted optimal cost at this point, i.e.

$$a(\bar{x}, \bar{b}, t) \equiv V(\bar{x}, \bar{b}, t) - \bar{V}(\bar{x}, \bar{b}, t) \tag{24}$$

Substituting Eq. (23)-(24) into eq. (22),

$$-\left\{\frac{\partial V}{\partial t} + \frac{\partial V_x}{\partial t}\delta x + \frac{\partial V_b}{\partial t}\delta b + \langle\delta x, \frac{\partial V_{xb}}{\partial t}\delta b\rangle + \frac{1}{2}\langle\delta x, \frac{\partial V_{xx}}{\partial t}\delta x\rangle + \frac{1}{2}\langle\delta b, \frac{\partial V_{bb}}{\partial t}\delta b\rangle\right\}$$

$$= \min_{\delta u}\left\{L + \langle V_x + \delta x' V_{xx} + \delta b' V_{xb}, f(\bar{x} + \delta x, \bar{u} + \delta u, t)\rangle\right\} \tag{25}$$

Because $V(x^*, b^*, t)$ is approximated by a second order expansion, the following relations between total and partial derivatives hold:

$$\frac{d}{dt}(\bar{V} + a) = \frac{\partial}{\partial t}(\bar{V} + a) + V_x f(\bar{x}, \bar{u}, t)$$

$$\frac{d}{dt} V_x = \frac{\partial V_x}{\partial t} + f'(\bar{x}, \bar{u}, t) V_{xx}$$

$$\frac{d}{dt} V_{xx} = \frac{\partial V_{xx}}{\partial t} \qquad (26)$$

$$\frac{d}{dt} V_b = \frac{\partial V_b}{\partial t} + f'(\bar{x}, \bar{u}, t) V_{bx}$$

$$\frac{d}{dt} V_{bb} = \frac{\partial V_{bb}}{\partial t}$$

$$\frac{d}{dt} V_{xb} = \frac{\partial V_{xb}}{\partial t}$$

All V and its partial derivatives are evaluated at $\bar{x}$, $\bar{b}$, t. Eq. (25) and (26) are fundamental equations in this DDP algorithm. From these equations we can identify all those partial derivatives of $V(\bar{x}, \bar{b}, t)$ in terms of the Hamiltonian, which we'll introduce next, and its partial derivatives with respect to u and x. These values can be computed simultaneously when we integrate Eq. (26) to find $V(\bar{x}, \bar{b}, t)$ and its partial derivatives with respect to x and b.

Finally, compute $V(x^*, b^*, t)$ according to Eq. (23). During this process, δu the optimal variation which should be added to the minimizing control $\bar{u}$ (which minimizes Hamiltonian) is also computed in terms of δx and δb.

Define the Hamiltonian to be

$$H(x, u, V_x, t) \equiv L(x, u, t) + V_x f(x, u, t) \qquad (27)$$

By this definition, if we let δx and δb be zero in the right hand side of Eq. (25), we have in terms of H

$$\min_{\delta u} \{H(\bar{x}, \bar{u} + \delta u, V_x, t)\} \tag{28}$$

First we can determine the optimal variation δu^* that minimizes the bracket in (28), and let the minimum be $H(\bar{x}, \tilde{u}, V_x, t)$ where $\tilde{u} = \bar{u} + \delta u^*$. The necessary conditions for this are

$$H_u(\bar{x}, \tilde{u}, V_x, t) = 0 \tag{29}$$

and

$$H_{uu}(x, \tilde{u}, V_x, t) > 0 \quad \text{(positive definite)}$$

This $\tilde{u}$ would be the optimal solution if the corresponding trajectory and multipliers were $\bar{x}$ and $\bar{b}$ respectively. However, this is not the case in general. Therefore, certain corrections on $\tilde{u}$ must be made to take into account the difference between $(\bar{x}, \bar{b})$ and the optimal one. Let these differences be δx and δb respectively. Reconsider the minimization of Hamiltonian as

$$\min_{\delta u} \{H(\bar{x} + \delta x, \tilde{u} + \delta u, V_x(\bar{x} + \delta x, \bar{b} + \delta b, t), t)\} \tag{30}$$

Again, necessary conditions for a minimum would be

$$\begin{aligned} &H_u(\bar{x} + \delta x, \tilde{u} + \delta u, V_x(\bar{x} + \delta x, \bar{b} + \delta b, t), t) = 0 \\ &H_{uu}(\bar{x} + \delta x, \tilde{u} + \delta u, V_x(\bar{x} + \delta x, \bar{b} + \delta b, t), t) > 0 \end{aligned} \tag{31}$$

In order to determine δu in terms of δx and δb, we expand Eq. (31) to first order about $\bar{x}$, $\tilde{u}$, $\bar{b}$, $\bar{t}$. Then

$$H_u' + H_{uu}\,\delta u + H_{ux}\,\delta x + f_u'(V_{xx}\,\delta x + V_{xb}\,\delta b) = 0$$

From Eq. (29) $H_u = 0$, hence

$$H_{uu}\,\delta u + (H_{ux} + f_u' V_{xx})\,\delta x + f_u' V_{xb}\,\delta b = 0$$

Assume $H_{uu}(\bar{x}, \tilde{u}, V_x, t)$ is nonsingular, then

$$\delta u = \beta_1 \, \delta x + \beta_2 \, \delta b \tag{32}$$

where $\beta_1 \equiv - H_{uu}^{-1} (H_{ux} + f_u' V_{xx})$

$$\beta_2 \equiv - H_{uu}^{-1} f_u' V_{xb} \tag{33}$$

Insert δu into Eq. (30) and expand it to second order about $\bar{x}$, $\tilde{u}$, $\bar{b}$, t; using the fact $H_u(\bar{x}, \tilde{u}, V_x, t) = 0$, we obtain

$$\begin{aligned} H + (H_x + f' V_{xx}) \, \delta x + f' V_{xb} \, \delta b + \langle \delta x, \{ (H_{ux} + f_u' V_{xx})' \beta_2 + \beta_1' H_{uu} \beta_2 \\ + (f_x + f_u \beta_1)' V_{xb} \} \, \delta b \rangle + \langle \delta b, \{ \tfrac{1}{2} \beta_2' H_{uu} \beta_2 + V_{xb}' f \beta_2 \} \, \delta b \rangle \\ + \langle \delta x, \{ \tfrac{1}{2} H_{xx} + V_{xx} f_x + \tfrac{1}{2} \beta_1' H_{uu} \beta_1 + \beta_1' (H_{ux} + f_u' V_{xx}) \} \, \delta x \rangle \end{aligned} \tag{34}$$

where all quantities are evaluated at $\bar{x}$, $\tilde{u}$, $\bar{b}$, t.

The series expansion (34) is now ready for identification with the left hand side of Eq. (25). We can identify those partial derivatives by equating the coefficients of power terms in δx and δb. Finally, after combining with Eq. (26) we obtain a set of ordinary differential equations from which V, V_x, V_b, V_{xb}, V_{xx}, V_{bb} are integrated; **i.e.**,

$$- \frac{da}{dt} = H - H(\bar{x}, \tilde{u}, V_x \, t)$$

$$- \frac{dV_x}{dt} = H_x + [f - f(\bar{x}, \tilde{u}, t)]' V_{xx}$$

$$- \frac{dV_b}{dt} = [f - f(\bar{x}, \tilde{u}, t)]' V_{xb}$$

$$-\frac{dV_{xb}}{dt} = [f_x + f_u\beta_1]' V_{xb} \tag{35}$$

$$-\frac{dV_{bb}}{dt} = -\beta_2' H_{uu} \beta_2$$

$$-\frac{dV_{xx}}{dt} = H_{xx} + f_x' V_{xx} + V_{xx} f_x + \beta_1' H_{uu} \beta_1 + \beta_1' (H_{ux} + f_u' V_{xx})$$

$$+ (H_{ux} + f_u' V_{xx})' \beta_1$$

with boundary conditions

$$a(\bar{x}(T), \bar{b}, T) = 0$$

$$V_x(\bar{x}(T), \bar{b}, T) = F_x(\bar{x}(T), T) + \bar{b}' \psi_x(\bar{x}(T), T)$$

$$V_b(\bar{x}(T), \bar{b}, T) = \psi'(\bar{x}(T), T) \tag{36}$$

$$V_{xb}(\bar{x}(T), \bar{b}, T) = \psi_x'(\bar{x}(T), T)$$

$$V_{bb}(\bar{x}(T), \bar{b}, T) = 0$$

$$V_{xx}(\bar{x}(T), \bar{b}, T) = F_{xx}(\bar{x}(T), T) + \bar{b}\, \psi_{xx}(\bar{x}(T), T)$$

All terms on the right hand side of Eq. (35) are evaluated at $\bar{x}$, $\tilde{u}$, $\bar{b}$, t unless other wise specified.

Table 1. Selected Rays and Radial Points

Ray No.	Polar Angle	x_1					x_2				
		E	D	C	B	A	E	D	C	B	A
1	0°	0.95	0.8	0.6	0.35	0.1	0.0	0.0	0.0	0.0	0.0
2	14°	0.92178	0.77624	0.5822	0.3396	0.9703	0.2298	0.1935	0.1452	0.0848	0.0242
3	30°	0.8227	0.6928	0.5196	0.3031	0.0866	0.4750	0.4	0.3	0.175	0.05
4	45°	0.6718	0.5657	0.4243	0.2475	0.0707	0.6718	0.5657	0.4243	0.2475	0.0707
5	68.2°	0.3526	0.2972	0.2229	0.1300	0.0372	0.8820	0.7427	0.5571	0.3245	0.0928
6	90°	0.0	0.0	0.0	0.0	0.0	0.95	0.8	0.6	0.35	0.1
7	105°	-0.2459	-0.2071	-0.1553	-0.0906	-0.0289	0.9176	0.7727	0.5796	0.3381	0.0966
8	120°	-0.4750	-0.4	-0.3	-0.175	-0.05	0.8227	0.6928	0.5196	0.3031	0.0866
9	135°	-0.6718	-0.5657	-0.4243	-0.2475	-0.0707	0.6718	0.5657	0.4243	0.2475	0.0707
10	150°	-0.8227	-0.6928	-0.5196	-0.3031	-0.0866	0.4750	0.4	0.3	0.175	0.05
11	165°	-0.9176	-0.7727	-0.5796	-0.3380	-0.0966	0.2459	0.2071	0.1553	0.0906	0.0259
12	180°	-0.95	-0.8	-0.6	-0.35	-0.1	0.0	0.0	0.0	0.0	0.0

Table 2. Lagrange Multipliers for Selected Radial Points

Radial Point	Launch Angle	Lagrange Multipliers		
		b_1	b_2	b_3
1 - E	120°	318.18433	22.61981	17.14204
	225°	234.19569	8.20671	14.46086
4 - D	60°	49.75749	27.24292	-6.63662
	-300°	29.18486	29.99333	-5.42888
6 - A	-270°	-2.22675	-2.06232	-0.16817
	-600°	-3.68478	-2.14910	-1.70457
9 - B	-200°	-0.28692	-3.63859	0.59244
	-360°	-4.60773	4.53999	0.98976
12 - C	-180°	-1.57937	-4.19836	0.88236
	-375°	-16.0	-0.8	0.05

Table 3. Feasible Ranges of Launching Angle

Point \ Ray	1		2	3	4	5	6	7	8	9	10	11	12	
A	-270°	270°*	270°	-270°	-270°	-270°	-270°	-270°	-270°	-270°	-270°	-270°	-270°	270°*
	-630°	630	630°	-630°	-630°	-630°	-630°	-630°	-630°	-630°	-630°	-630°	-630°	630°
B	-210°	210°	240°	-210°	-210°	-210°	-210°	-210°	-210°	-210°	-210°	-210°	-210°	210°
	-570°	570°	600°	-570°	-570°	-600°	-570°	-570°	-570°	-570°	-570°	-480°	-540°	540°
C	-90°	90°	0°	-150°	-150°	-150°	-180°	-150°	-150°	-150°	-150°	-150°	-150°	150°
	-450°	450°	360°	-510°	-510°	-510°	-540°	-510°	-510°	-510°	-450°	-390°	-375°	375°
D	-45°	45°	30°	0°	0°	-30°	-90°	-90°	-120°	-120°	-90°	-90°	-120°	120°
	-405°	405°	390°	-360°	-300°	-390°	-450°	-450°	-360°	-330°	-330°	-360°	-300°	300°
E	120°	-120°	-270°	-60°	0°	40°	60°	90°	120°	-30°	-90°	-50°	-60°	60°
	225°	-225°	-300°	-330°	-330°	-290°	-270°	-270°	-210°	-190°	-210°	-180°	-180°	180°

*Feasible ranges of launching angle according to x_1-axis symmetry. See Section II.C.

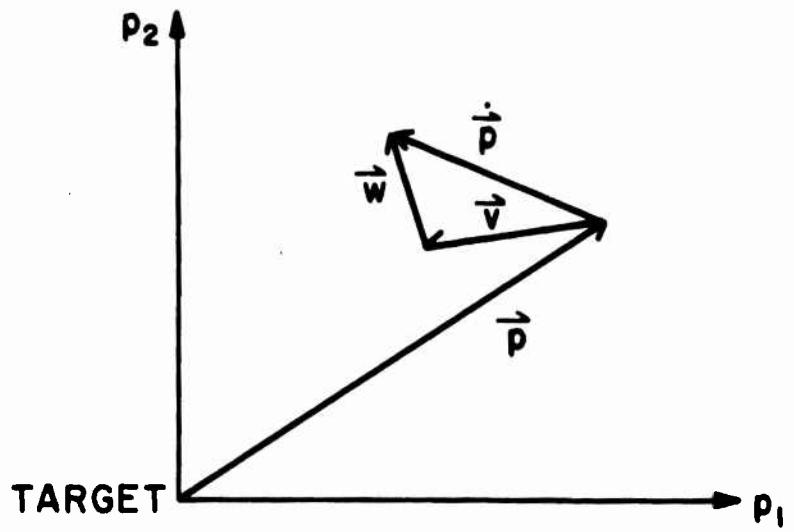

FIG. 1 PARACHUTE DYNAMICS IN HORIZONTAL PLANE.

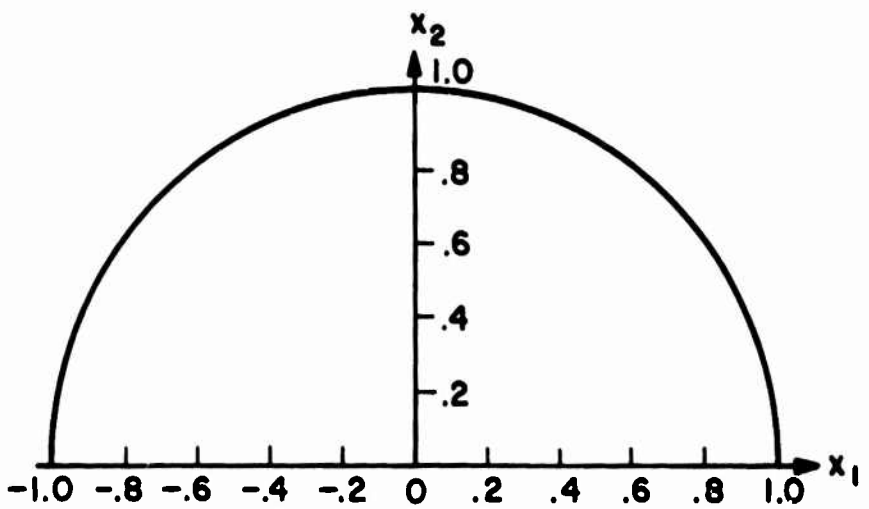

FIG. 2 UPPER HALF UNIT CIRCLE.

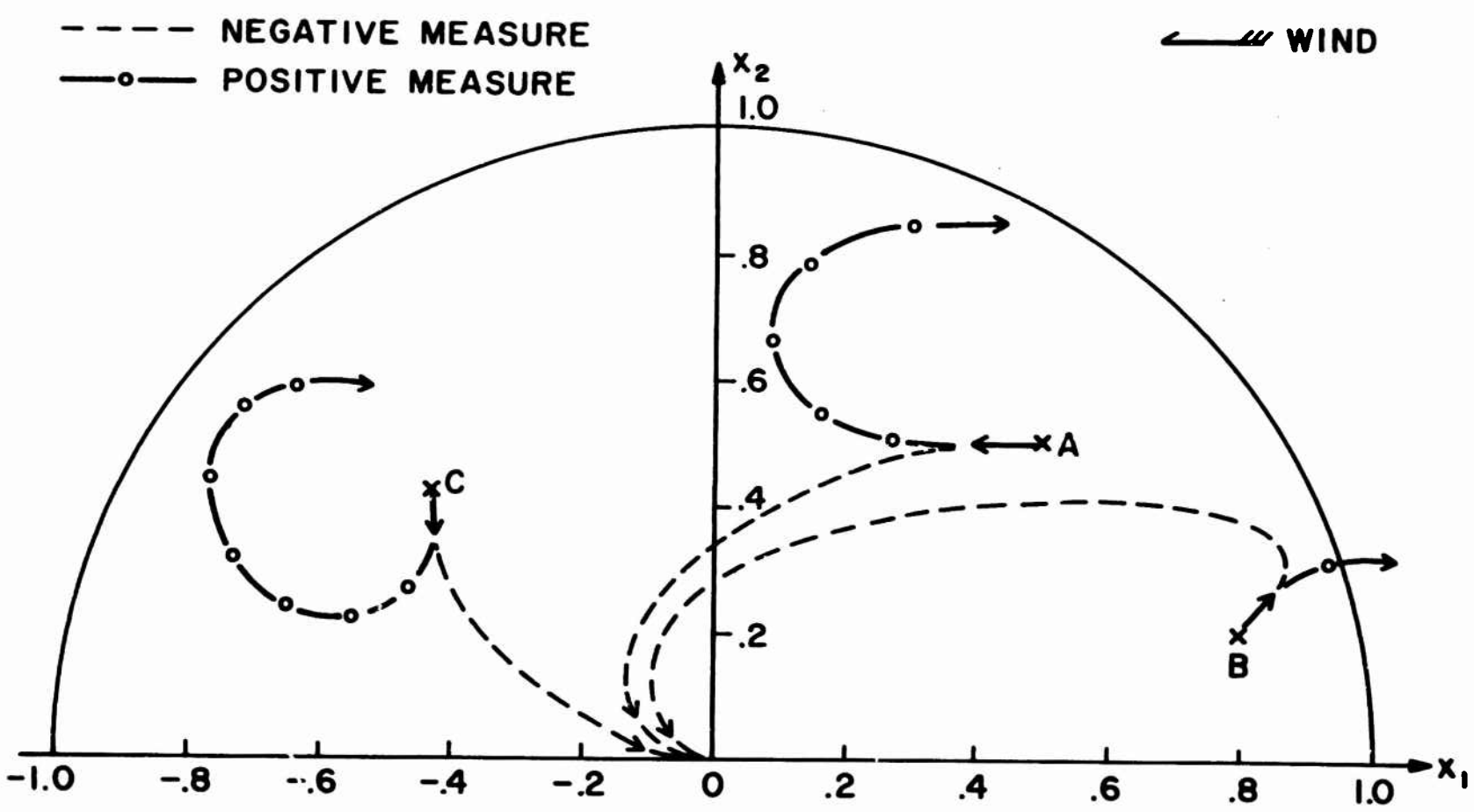

FIG. 3 TENTATIVE OPTIMAL TRAJECTORIES FOR DIFFERENT MEASUREMENT OF THE LAUNCHING ANGLE.

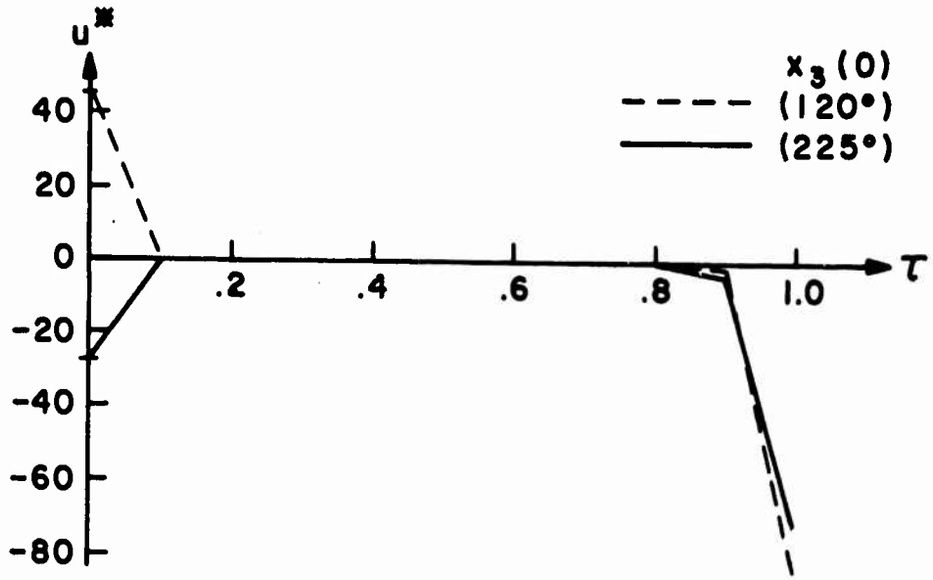

FIG. 4(a) OPTIMAL CONTROLS VS. NORMALIZED TIME.

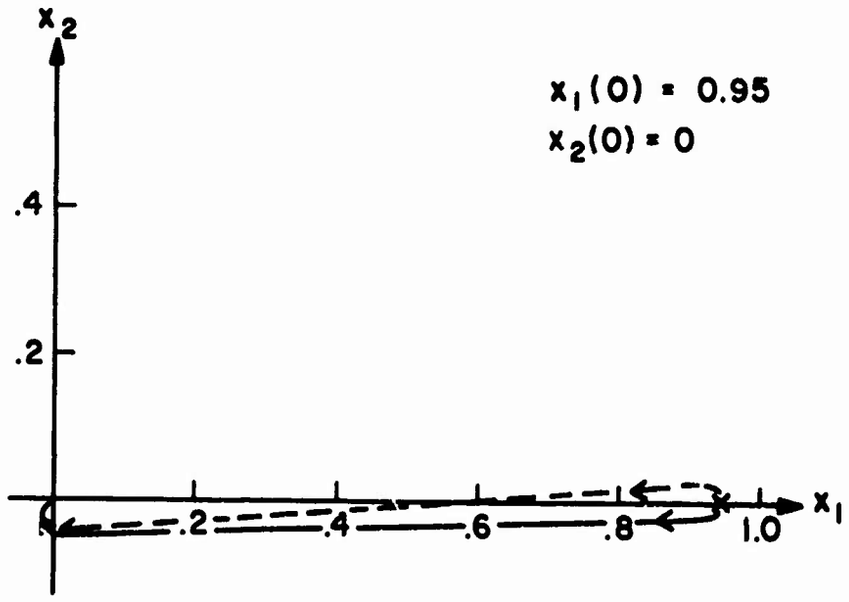

FIG. 4(b) OPTIMAL TRAJECTORIES IN NORMALIZED COORDINATES.

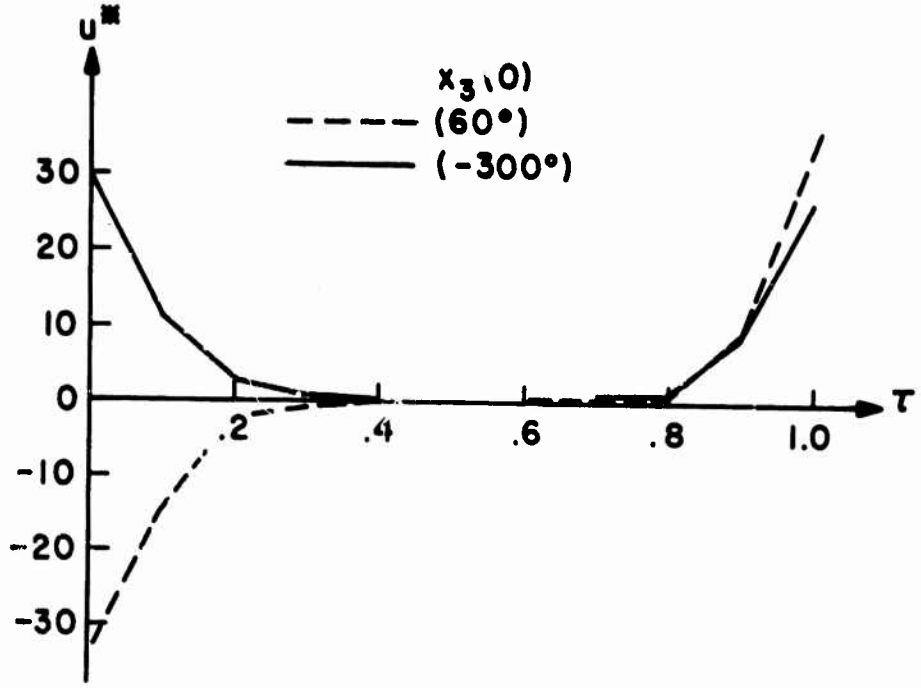

FIG. 5(a) OPTIMAL CONTROLS VS. NORMALIZED TIME.

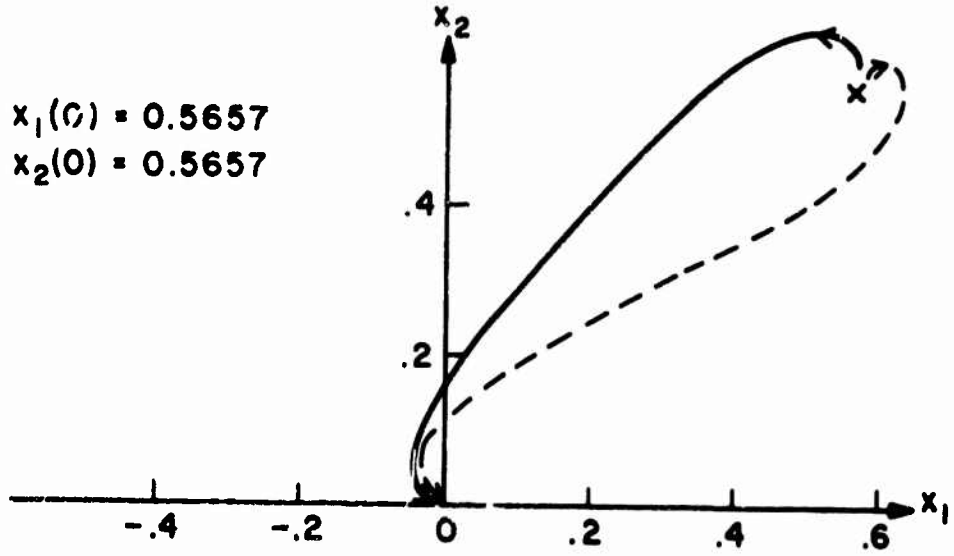

FIG. 5(b) OPTIMAL TRAJECTORIES IN NORMALIZED COORDINATES.

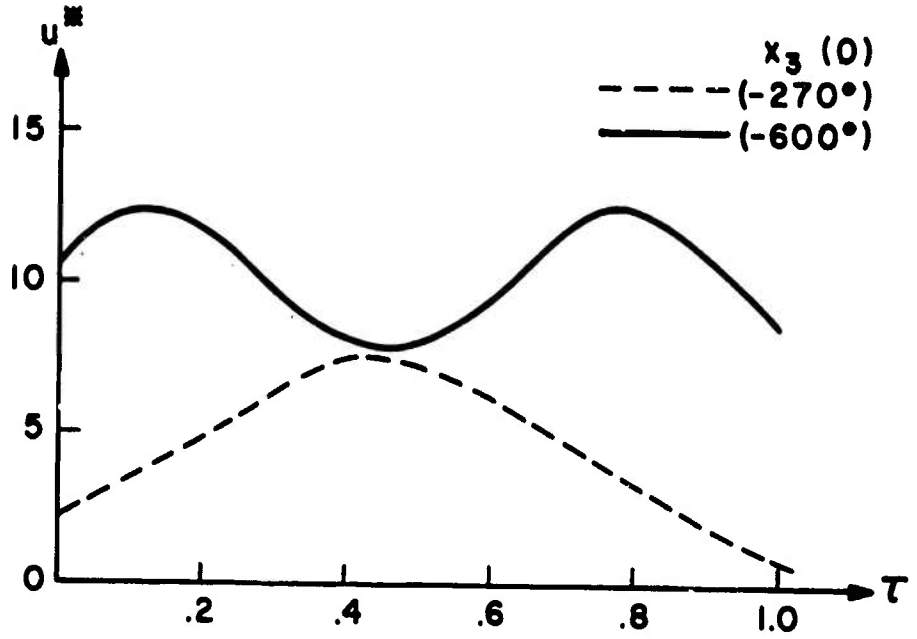

FIG. 6(a) OPTIMAL CONTROLS VS. NORMALIZED TIME.

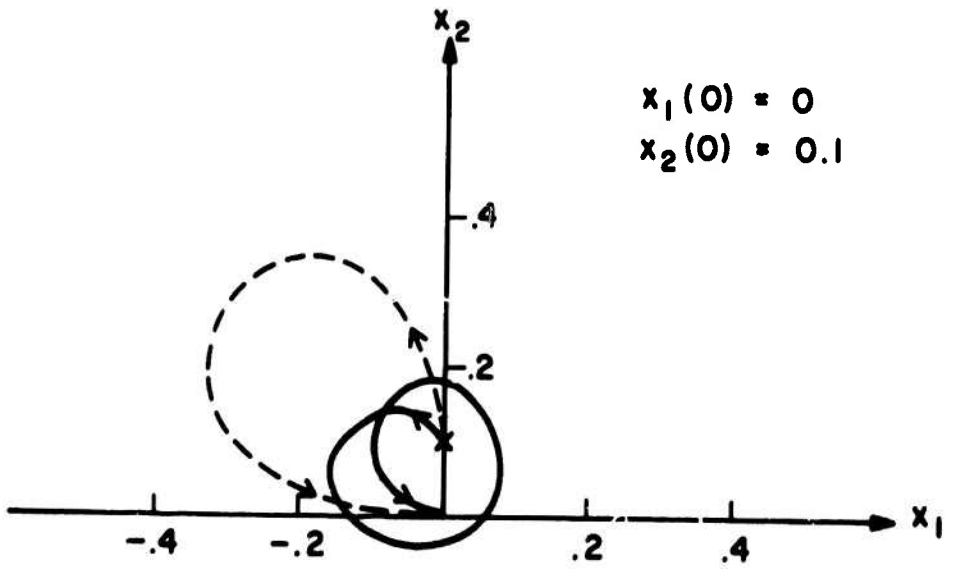

FIG. 6(b) OPTIMAL TRAJECTORIES IN NORMALIZED COORDINATES.

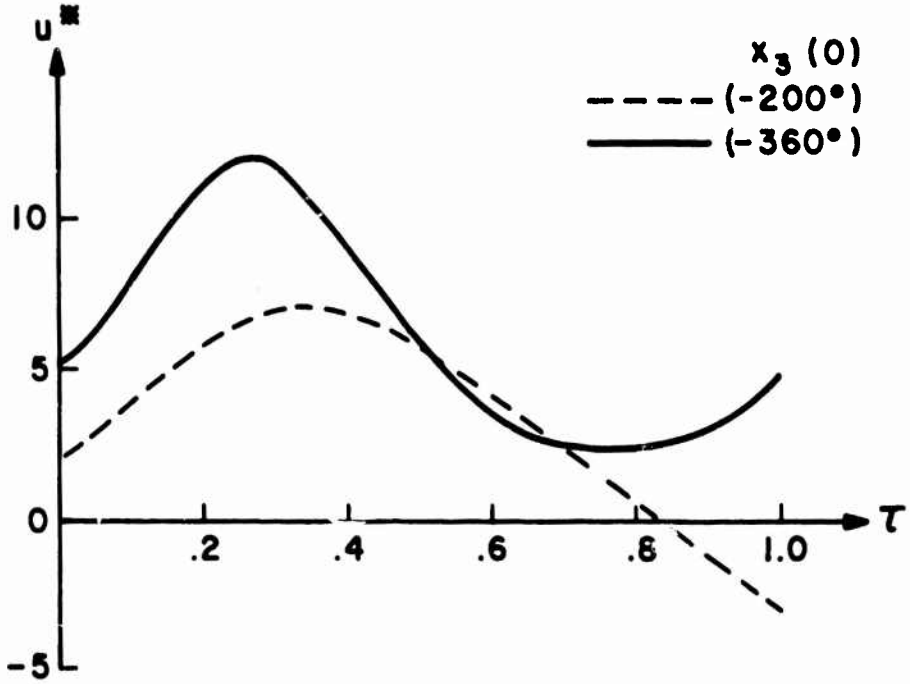

FIG. 7(a) OPTIMAL CONTROLS VS. NORMALIZED TIME.

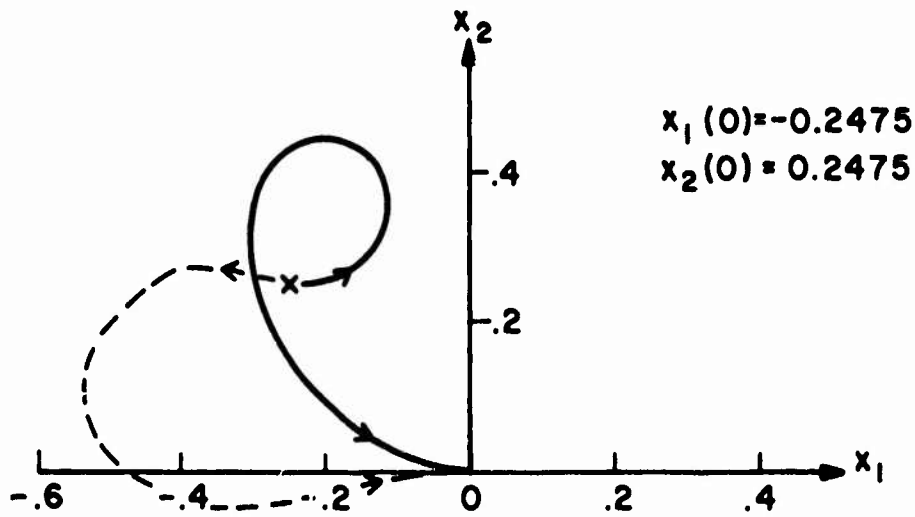

FIG. 7(b) OPTIMAL TRAJECTORIES IN NORMALIZED COORDINATES.

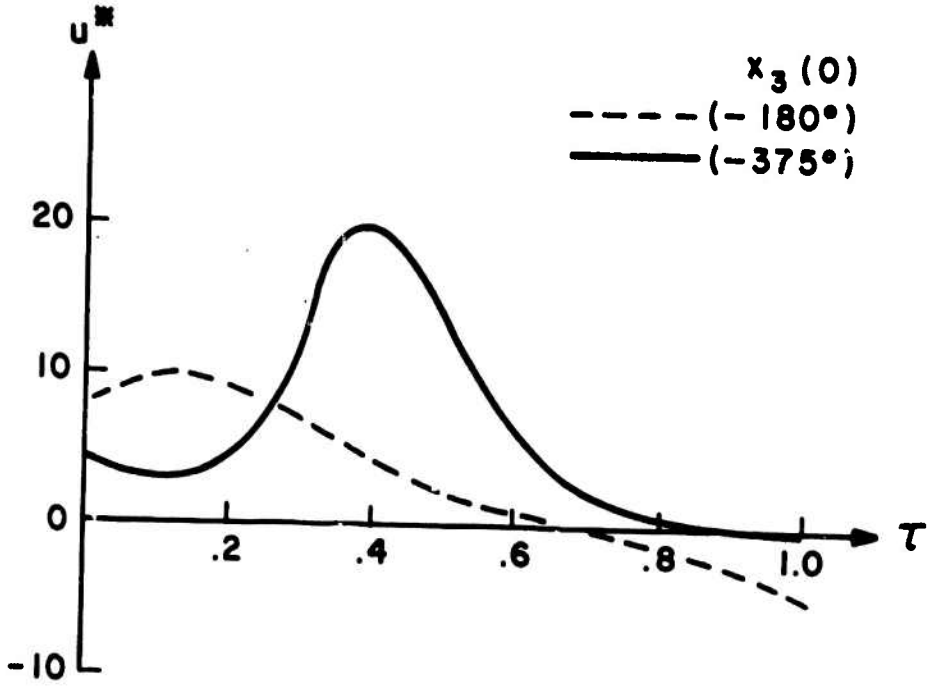

FIG. 8(a) OPTIMAL CONTROLS VS. NORMALIZED TIME.

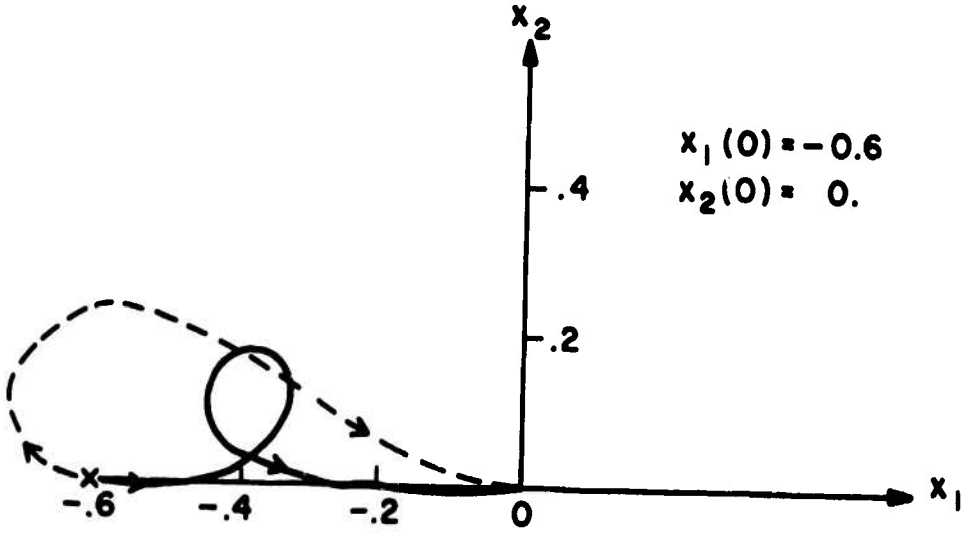

FIG. 8(b) OPTIMAL TRAJECTORIES IN NORMALIZED COORDINATES.

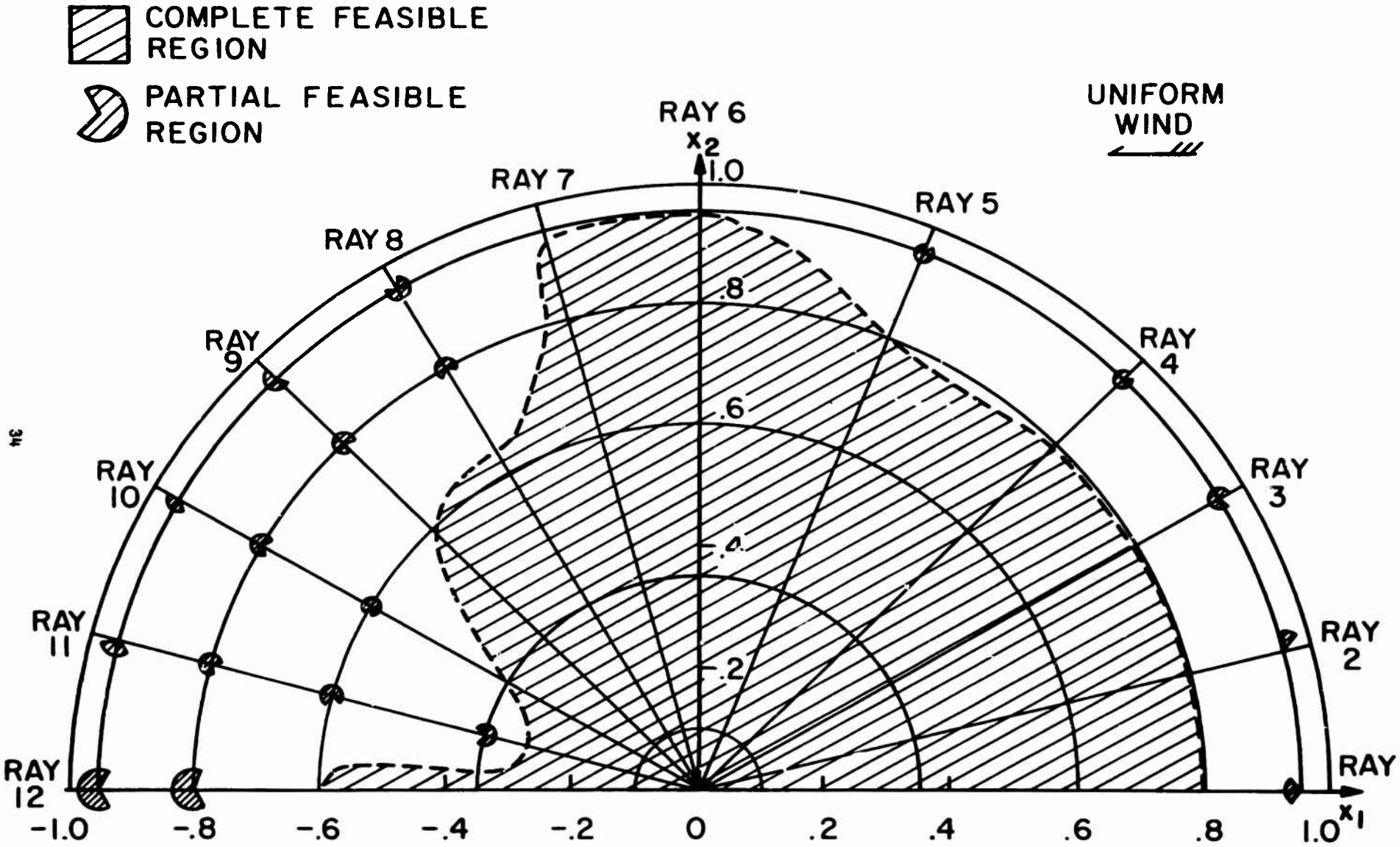

FIG. 9 A SUMMARY CHART OF FEASIBLE REGION IN THE UPPER HALF UNIT CIRCLE

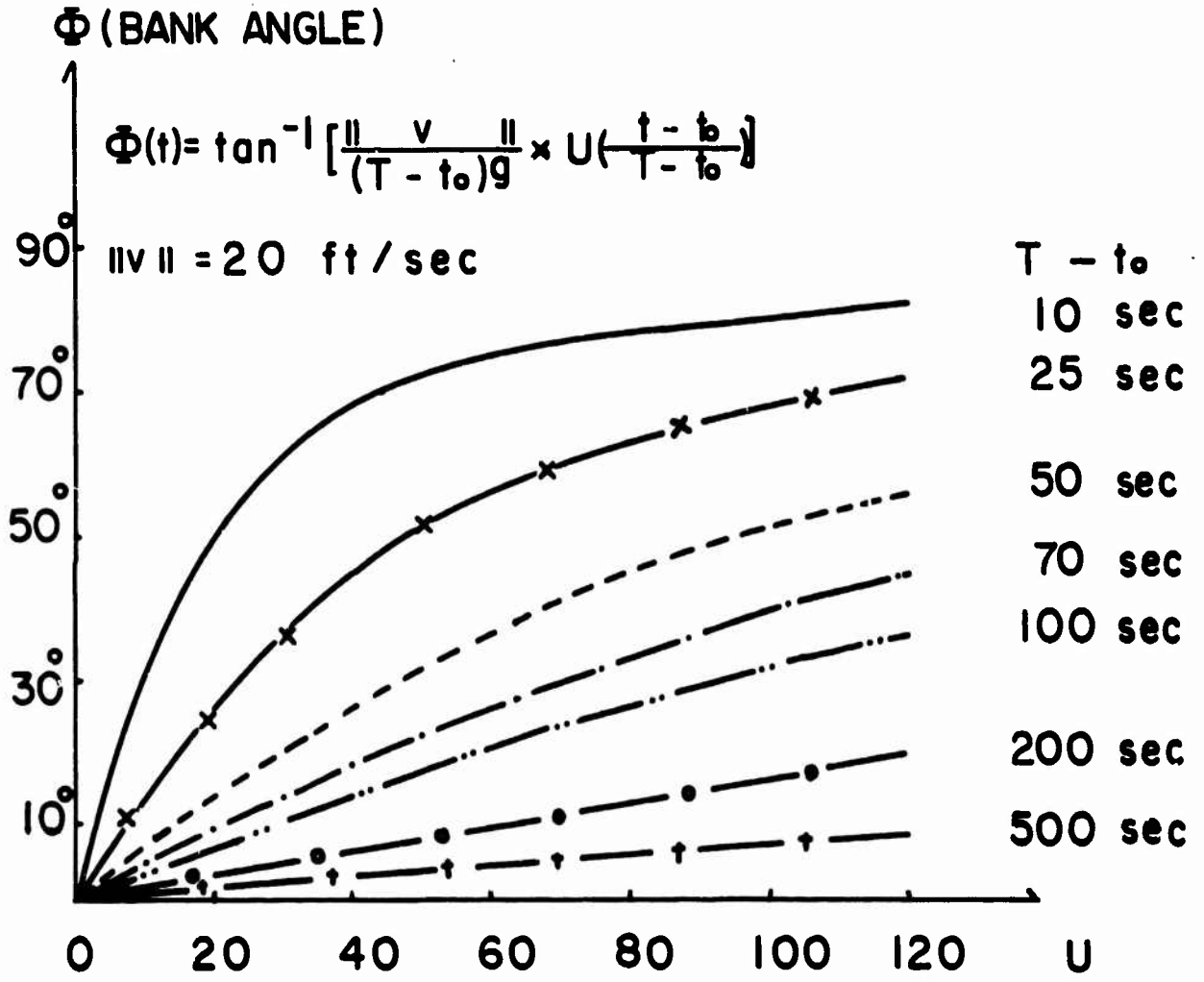

FIG. 10 BANK ANGLE vs NORMALIZED CONTROL